

## Articles

## Sequence and Structure Dependence of the Hybridization-Triggered Reaction of Oligonucleotides Bearing Conjugated Cyclopropapyrroloindole

Eugeny A. Lukhtanov,\* Igor V. Kutyavin, Vladimir V. Gorn, Michael W. Reed, A. David Adams, Deborah D. Lucas, and Rich B. Meyer, Jr.

Contribution from Epoch Pharmaceuticals, Inc., 1725 220th Street Southeast, #104, Bothell, Washington 98021

Received January 29, 1997<sup>⊗</sup>

**Abstract:** Oligodeoxyribonucleotides (ODNs) with conjugated reactive groups are potential sequence-specific gene inactivating agents. The antitumor antibiotic CC-1065 binds preferably in the minor groove of A-T-rich sites of double-stranded DNA, and the cyclopropapyrroloindole (CPI) subunit of the drug alkylates adenines at their N3 position. Pure enantiomeric (+)- and (–)-CPI and its N5-methyl homologue (MCPI) were synthesized and conjugated to an ODN. These conjugates were evaluated for their ability to alkylate a target containing a duplex region immediately adjacent to a single-stranded complementary binding region for the ODN conjugate. The conjugates demonstrated excellent stability in physiologic conditions and stereospecific, hybridization-triggered alkylation of the synthetic ODN targets. The dependence of the reaction rates on sequence of the duplex target region was in accord with the predicted minor groove binding of the conjugated CPI. The reactivity was highly dependent on the structure of the cross-linking group. Natural (+)-enantiomers alkylate 10–20 times faster than the corresponding (–)-enantiomers. Regiospecificity of the alkylation reaction is conferred by the length of the spacer arm. N5-Methylation of the CPI moiety suppresses the reactivity by a factor of 3–5. Addition of a 1,2-dihydro-3H-pyrrolo-[3,2-*e*]indole-7-carboxylate (DPI) binding subunit of CC-1065 between CPI or MCPI residues and an ODN results in a significant enhancement of the reactivity which is especially pronounced for (–)-enantiomers. The main products of sequence-specific alkylation were determined for complexes with the most efficient reactions.

## Introduction

Direct and specific modification of gene function could provide a general approach to treatment of many diseases. Efficiency and selectivity of action can be achieved by synthetic oligodeoxynucleotides (ODNs) which are able to form complementary complexes with preselected sequences of double-stranded DNA (the antigene approach) or mRNA (the antisense approach). Although development of antisense ODNs is well into the clinical stage,<sup>1</sup> ODNs that target DNA have barriers that have hindered their development. Lacking the ability to catalyze the degradation of the target, as most antisense ODNs do via RNase H action, DNA-directed ODNs must either bind very tightly or carry a DNA modifying group to attain efficacy of action.

We have been concentrating on achieving modification of gene function with use of ODNs bearing an alkylating group. While the therapeutic utility of these agents shares some of the hurdles facing antisense ODNs, such as cell uptake and sensitivity of the phosphodiester backbone to nucleases, the properties of the reactive group add unique considerations. A large number of studies have been directed toward enhancing stabilization of the backbone,<sup>2</sup> but the stability of the reactive group remains an important issue. For example, ODNs deriva-

tized with (haloacetamido)alkyl groups<sup>3,4</sup> or aromatic 2-chloroethylamines (mustards) such as *p*-(*N*-(2-chloroethyl)-*N*-methyl)-benzyl<sup>5</sup> and chlorambucil<sup>6,7</sup> have been shown to alkylate complementary DNA targets with high efficiency and sequence specificity. ODNs bearing haloacetamides have limited application in cellular systems due to their inherent reactivity, both with themselves and with nontarget cellular nucleophiles prior to nucleic acid binding. The mustards offer advantages in reactivity due to their spontaneous activation,<sup>8</sup> but may still react at nontarget sites.

The most attractive way to address the selectivity problem is to use hybridization-triggered agents, which are chemically stable when conjugated to a single-stranded ODN, but highly activated after hybridization of the ODN to DNA target. Matteucci and co-workers investigated *N*<sup>4</sup>-ethanocytosine-containing ODNs as hybridization triggered electrophiles,<sup>9–11</sup>

(3) Tabone, J. C.; Stamm, M. R.; Gamper, H. B.; Meyer, R. B. *Biochemistry* **1994**, *33*, 375–383.

(4) Povsic, T. J.; Dervan, P. B. *J. Am. Chem. Soc.* **1990**, *112*, 9428–9430.

(5) Knorre, D. G.; Vlassov, V. V. *Prog. Nucleic Acids Res. Mol. Biol.* **1985**, *32*, 291–320.

(6) Kutyavin, I. V.; Gamper, H. B.; Gall, A. A.; Meyer, R. B. *J. Am. Chem. Soc.* **1993**, *115*, 9303–9304.

(7) Podyminogin, M. A.; Meyer, R. B.; Gamper, H. B. *Biochemistry* **1995**, *34*, 13098–13108.

(8) Knorre, D. G.; Vlassov, V. V. *Genetica* **1991**, *85*, 53–63.

(9) Webb, T. R.; Matteucci, M. D. *J. Am. Chem. Soc.* **1986**, *108*, 2764–2765.

\* Corresponding author. Telephone: 206-485-8566. Facsimile: 206-486-8336. E-mail: elukhtan@epochpharm.com.

<sup>⊗</sup> Abstract published in *Advance ACS Abstracts*, July 1, 1997.

(1) Croke, S. T.; Bennett, C. F. *Annu. Rev. Pharmacol. Toxicol.* **1996**, *36*, 107–129.

(2) Cook, P. D. *Anticancer Drug Des.* **1991**, *6*, 585–607.

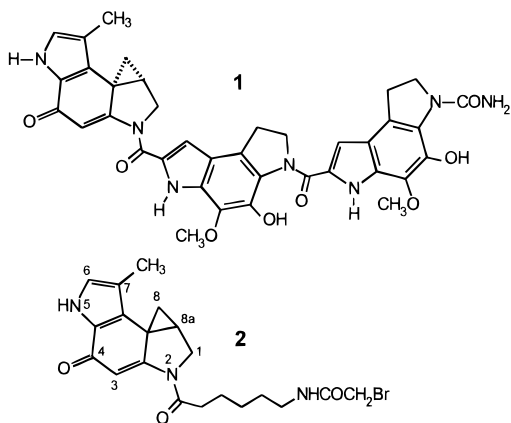


**Figure 1.** Structures of (+)-CC-1065 (**1**) and (*N*<sup>6</sup>-(bromoacetyl)amino)hexanoyl CPI (**2**).

but they are slow in the cross-linking reaction, with a half-life of approximately 30 h. The alkylated base was a mismatched cytosine. Rokita et al. used a stable silylated phenolic quinone methide precursor,<sup>12</sup> which upon hybridization, lost the silyl group to generate the reactive species. Alkylation of the complementary strand occurred with moderate efficiency over several hours.

We have recently developed<sup>13</sup> a new class of hybridization-triggered cross-linking ODNs using a conjugated cyclopropapyrroloindole (CPI) subunit derived from the potent antitumor antibiotic (+)-CC-1065<sup>14</sup> (**1**) (Figure 1). This reactive CPI subunit is responsible for the N3 alkylation of adenine.<sup>15</sup> CC-1065 is very stable in neutral aqueous solution<sup>16,17</sup> but becomes much more reactive when bound to the minor groove of double-stranded DNA. The precise mechanism of activation of the cyclopropane function is not clear. Catalytic effects such as DNA-mediated general acid catalysis (protonation of C4 carbonyl)<sup>18,19</sup> or alkylation site catalysis<sup>20</sup> have been proposed, as have the conformational effects of DNA-induced bond strain on the CPI moiety.<sup>21,22</sup> The activation involves a high-affinity minor groove binding interaction, which is strengthened by the middle and right-hand subunits. The DNA alkylation occurs with sequence dependence, with a preference to 5'-PuNTTA\* and 5'-AAAAA\*, where \* marks the preferred alkylation site.<sup>23,24</sup>

(10) Webb, T. R.; Matteucci, M. D. *Nucleic Acids Res.* **1986**, *14*, 7661–7674.

(11) Shaw, J.-P.; Milligan, J. F.; Krawczyk, S. H.; Matteucci, M. J. *Am. Chem. Soc.* **1991**, *113*, 7765–7766.

(12) Li, T.; Zeng, Q.; Rokita, S. E. *Bioconjugate Chem.* **1994**, *5*, 497–500.

(13) Lukhtanov, E. A.; Podyminogin, M. A.; Kutuyavin, I. V.; Meyer, R. B.; Gamber, H. B. *Nucleic Acids Res.* **1996**, *24*, 683–687.

(14) Reynolds, V. L.; McGovren, J. P.; Hurley, L. H. *J. Antibiotics (Tokyo)* **1986**, *39*, 319–334.

(15) Hurley, L. H.; Reynolds, V. L.; Swenson, D. H.; Petzold, G. L.; Scahill, T. *Science* **1984**, *226*, 843–844.

(16) Warpehoski, M. A.; Gebhard, I.; Kelly, R. C.; Krueger, W. C.; Li, L. H.; McGovren, J. P.; Prairie, M. D.; Wicnienski, N.; Wierenga, W. J. *Med. Chem.* **1988**, *31*, 590–603.

(17) Warpehoski, M. A.; Harper, D. E. *J. Am. Chem. Soc.* **1994**, *116*, 7573–7580.

(18) Warpehoski, M. A.; Hurley, L. H. *Chem. Res. Toxicol.* **1988**, *1*, 315–333.

(19) Lin, C. H.; Beale, J. M.; Hurley, L. H. *Biochemistry* **1991**, *30*, 3597–3602.

(20) Warpehoski, M. A.; Harper, D. E. *J. Am. Chem. Soc.* **1995**, *117*, 2951–2952.

(21) Boger, D. L.; Boyce, C. W.; Johnson, D. S. *Bioorg. Med. Chem. Lett.* **1997**, *7*, 233–238.

(22) Boger, D. L.; Garbaccio, R. M. *Bioorg. Med. Chem.* **1997**, *5*, 263–276.

(23) Reynolds, V. L.; Molineux, I. J.; Kaplan, D. J.; Swenson, D. H.; Hurley, L. H. *Biochemistry* **1985**, *24*, 6628–6237.

In our initial approach<sup>13</sup> to design a sequence-specific, hybridization-triggered ODN reagent, we conjugated racemic CPI to a 3'-thiophosphate tailed ODN using CPI reagent **2** (Figure 1). The sequence of the ODN reagent and complementary single-stranded target was designed in such a way that, after hybridization, the CPI moiety would be directed to adenines of the target. Indeed, 3'-CPI-ODN conjugate was found to alkylate the complement, which contained an A<sub>6</sub> run immediately next to its 5' end, very rapidly and efficiently. In the present study, we have further investigated (i) the effect of sequence of the target site on the efficiency of alkylation, (ii) specificity and efficiency of alkylation by purified conjugated CPI enantiomers, (iii) the effect of the linker connecting an ODN and the CPI moiety, and (iv) whether efficient alkylation could be maintained with reduced propensity for side reactions. A new type of CPI reagent, N5-methyl CPI (MCPI), was developed to modulate the powerful reactivity of CPI. The structure–activity studies reported here address these questions and establish the effect of N5-methylation on CPI reactivity.

## Results and Discussion

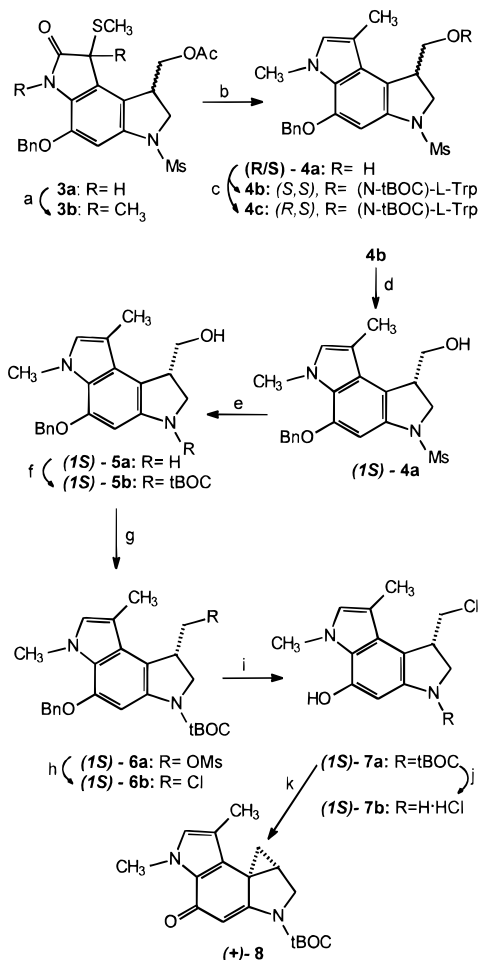
**Synthesis of MCPI and CPI Derivatives.** The synthetic approach to the preparation of the chloromethyl compound (**7a**), the key intermediate of new MCPI analogues, is shown in Scheme 1. Oxindole **3a** was exhaustively methylated, affording bis-methylated oxindole **3b**. Borane–methyl sulfide reduction<sup>16</sup> gave racemic MCPI precursor **4a** in 80% yield from **3a**. Esterification of the primary alcohol **4a** with *N*-BOC-L-tryptophan<sup>25</sup> afforded a mixture of diastereomeric esters **4b,c**. The (*S,S*) diastereomer **4b** was selectively crystallized from hexane/ethyl acetate in 50–60% yield. (*R,S*)-Diastereomer **4c** was isolated from the mother liquor by preparative chromatography on silica. Methanolysis of **4b** afforded 99% pure alcohol (*1S*)-**4a** with *1S* absolute configuration (natural configuration of (+)-CC-1065). This assignment was later unequivocally proved by the difference observed in the DNA alkylating properties of MCPI agents with opposite absolute configuration. All of the following steps were performed analogously for each enantiomer. Red-Al removal of the methanesulfonyl group gave unstable dihydrobenzodipyrrole **5a**, which was not purified but reacted directly with di-*tert*-butyl dicarbonate to provide the protected N3-BOC dihydrobenzodipyrrole **5b**. A two-step reaction,<sup>25</sup> involving the transient formation of mesylate **6a** followed by chloride substitution, provided the 1-chloromethyl intermediate **6b**. Finally, debenzoylation by phase transfer catalysis gave the desired intermediate **7a**. The analogous CPI intermediate (**15a**) (Scheme 3) was synthesized as previously described.<sup>16,24,26</sup>

To prepare CPI derivatives suitable for further conjugation with an ODN, we employed two general synthetic routes. In the first case (method A), reactive haloacetamide groups, suitable for coupling with a thiophosphate on the ODN, were incorporated into the CPI residue directly at the N2 position or via variable in length linkers as shown on Scheme 2. The synthesis of haloacetamido derivatives **11b**, **12b**, and **14** proceeded from unstable indoline hydrochloride **7b**, prepared by treatment of **7a** with saturated HCl in ethyl acetate. Coupling of **7b** and *N*-BOC-aminohexanoic acid or *N*-BOC-aminopropanoic acid in the presence of *N*-(3-(dimethylamino)propyl)-*N'*-ethylcarbodi-

(24) Hurley, L. H.; Warpehoski, M. A.; Lee, C. -S.; McGovren, J. P.; Scahill, T. A.; Kelly, R. C.; Mitchell, M. A.; Wicnienski, N. A.; Gebhard, I.; Johnson, P. D.; Bradford, V. S. *J. Am. Chem. Soc.* **1990**, *112*, 4633–4649.

(25) Warpehoski, M. A. *Tetrahedron Lett.* **1986**, *27*, 4103–4106.

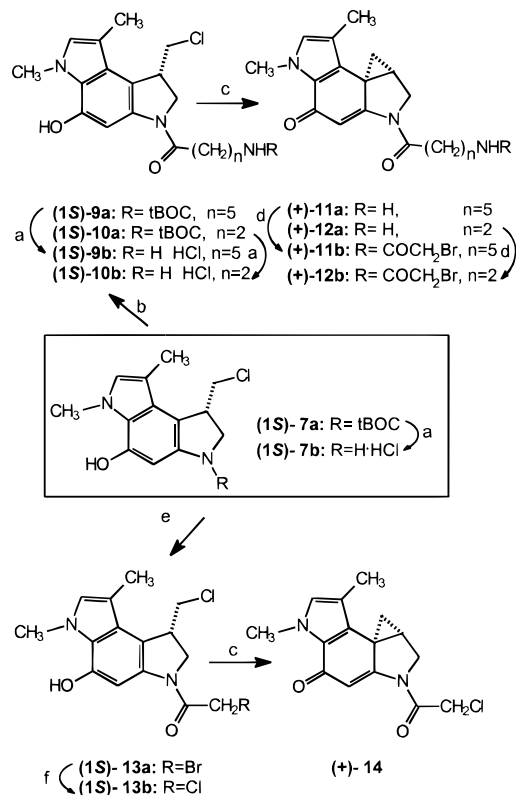
(26) Kelly, R. C.; Gebhard, I.; Wicnienski, N.; Aristoff, P. A.; Johnson, P. D.; Martin, D. G. *J. Am. Chem. Soc.* **1987**, *109*, 6837–6838.

**Scheme 1.** Synthesis of MCPI Precursors<sup>a</sup>

<sup>a</sup> Reagents: (a) CH<sub>3</sub>I, Na<sub>2</sub>CO<sub>3</sub>, acetone, DMF; (b) BH<sub>3</sub>·(CH<sub>3</sub>)<sub>2</sub>S, THF; (c) *N*-BOC-L-tryptophan, DCC, *N*-methylimidazole, 1,4-dioxane; (d) NaOCH<sub>3</sub>, MeOH; (e) Red-Al, THF, toluene; (f) di-*tert*-butyl dicarbonate, THF; (g) CH<sub>3</sub>SO<sub>2</sub>Cl, pyridine, CH<sub>2</sub>Cl<sub>2</sub>; (h) LiCl, DMF; (i) 10% Pd/C, NH<sub>4</sub>COOH, THF, MeOH; (j) HCl/EtOAc; (k) Et<sub>3</sub>N, CH<sub>3</sub>CN, H<sub>2</sub>O.

imide hydrochloride (EDC) (Scheme 2) afforded compound **9a** or **10a**, respectively. The hydrochlorides **9b** and **10b** obtained from **9a** and **10a** were treated with 1:1:3 Et<sub>3</sub>N/H<sub>2</sub>O/CH<sub>3</sub>CN to effect Ar-3' spirocyclization<sup>26</sup> (**11a** and **12a**). Final coupling with *N*-hydroxysuccinimidy bromoacetate afforded the desired MCPI-bromoacetamido derivatives **11b** and **12b** in 50% overall yield from **7b**. When **7b** was coupled with bromoacetic acid in presence of EDC (Scheme 2), the bromoacetamide **13a** was not obtained. Chloroacetamide **13b** was isolated instead from the reaction mixture as a result of halogen exchange driven by the excess chloride ion (EDC counterion). Although the reaction scheme could be modified to avoid using the excess chloride ion, chloroacetamido MCPI **14**, prepared from **13b** using the standard cyclization conditions, proved to be reactive enough in the following conjugation reaction with the nucleophilic ODN.

An alternative conjugation method (method B) is to use CPI and MCPI derivatives bearing a linker with activated carboxy group to be coupled to an amine tailed ODN. For use in this method (Scheme 3), **7b** (or **15b**)<sup>24</sup> was selectively derivatized with succinic anhydride, providing succinate **16** (or **17**) followed by Ar-3' spirocyclization as described above to afford succinate **18a** (or **19a**). Activation of the terminal carboxy group using

**Scheme 2.** Synthesis of Haloacetamide Intermediates<sup>a</sup>

<sup>a</sup> Reagents: (a) HCl/EtOAc; (b) (*N*-BOC-amino)hexanoic acid or (*N*-BOC-amino)propanoic acid, EDC, DMA; (c) Et<sub>3</sub>N, CH<sub>3</sub>CN, H<sub>2</sub>O; (d) bromoacetic acid *N*-hydroxysuccinimide, DMF; (e) bromoacetic acid, EDC; (f) Cl<sup>-</sup>.

2,3,5,6-tetrafluorophenyl (TFP) trifluoroacetate<sup>27</sup> gave MCPI-TFP ester (**18b**) (37% overall yield from **7a**) or CPI-TFP ester (**19b**) (44% overall yield from **15a**). MCPI-DPI (DPI = 1,2-dihydro-3*H*-pyrrolo[3,2-*e*]indole-7-carboxylate) (**22b**) and CPI-DPI (**23b**) TFP esters were prepared in a manner identical with that described for **18b** and **19b**, except that addition of the DPI fragment was accomplished using EDC-mediated coupling of **7b** (or **15b**) with BOC-DPI.<sup>28</sup> UV characteristics of the new derivatives are summarized in Table 1.

**Solvolytic Reactivity of MCPI.** An important characteristic of CC-1065 alkylating subunit and related analogues is the pH-rate profile for solvolysis. These reagents undergo acid-catalyzed ring opening with nucleophilic addition to the least substituted cyclopropane carbon.<sup>17,29</sup> Comparison of a series of agents possessing a modified CC-1065 alkylating subunit has shown that the rate of acid-catalyzed hydrolysis directly correlates with biological potency.<sup>29,30</sup> The more potent of these agents are also the most stable and take best advantage of the selectivity achieved by DNA binding-induced reactivity enhancement.<sup>31</sup>

We determined the solvolytic reactivity of the cyclopropyl function in our compounds. Model *N*-BOC protected analogue **8** (*N*-BOC-MCPI), whose reactivity could be directly compared

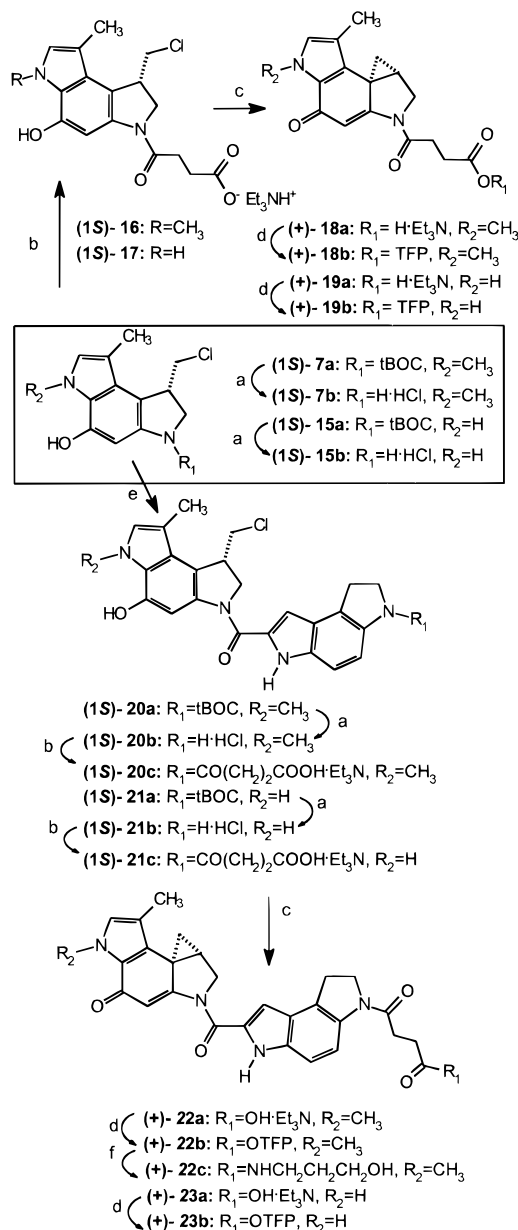
(27) Gamper, H. B.; Reed, M. W.; Cox, T.; Viroso, J. S.; Adams, A. D.; Gall, A. A.; Scholler, J. K.; Meyer, R. B., Jr. *Nucleic Acids Res.* **1993**, *21*, 145–150.

(28) Boger, D. L.; Coleman, R. S.; Invergo, B. J. *J. Org. Chem.* **1987**, *52*, 1521–1530.

(29) Boger, D. L.; Machiya, K.; Hertzog, D. L.; Kitos, P. A.; Holmes, D. *J. Am. Chem. Soc.* **1993**, *115*, 9025–9036.

(30) Boger, D. L.; Johnson, D. S. *Angew. Chem., Int. Ed. Engl.* **1996**, *35*, 1439–1474.

(31) Boger, D. L.; Johnson, D. S. *Proc. Natl. Acad. Sci. U.S.A.* **1995**, *92*, 3642–3649.

**Scheme 3.** Synthesis of TFP Intermediates<sup>a</sup>

<sup>a</sup> Reagents: (a) HCl/EtOAc; (b) succinic anhydride, Et<sub>3</sub>N, (MeOH, CH<sub>2</sub>Cl<sub>2</sub>) or DMA; (c) Et<sub>3</sub>N, CH<sub>3</sub>CN, H<sub>2</sub>O; (d) 2,3,5,6-tetrafluorophenyl trifluoroacetate, Et<sub>3</sub>N, CH<sub>2</sub>Cl<sub>2</sub>, or DMA; (e) 3-(*tert*-butyloxycarbonyl)-1,2-dihydro-3*H*-pyrrolo[3,2-*c*]indole-7-carboxylic acid, EDC, DMA; (f) 3-aminopropanol, DMF.

with other *N*-BOC-protected CPI analogues,<sup>29</sup> was synthesized as shown in Scheme 1. Compound **8** was found to have a half-life of 35.8 h ( $k = 5.38 \times 10^{-6} \text{ s}^{-1}$ ) at pH 4 (22 °C) and was about as stable as the natural analogue *N*-BOC-CPI ( $t_{1/2} = 36.7 \text{ h}$ <sup>29</sup>). This shows that N5-methylation has negligible effect on the electronic properties of the aromatic system and on the  $pK_a$  of the C4 oxygen protonated in the acid-catalyzed reaction. This is also supported by the fact that both *N*-methylated (**18b**) and natural (**19b**) CPI analogues have remarkably similar UV spectra (Table 1). This observation is interesting in a context of the comparative reactivities of corresponding CPI and MCPI-carrying ODN conjugates in reaction with complementary targets discussed below.

**Conjugation Chemistry.** Two types of conjugation chemistries were used to couple an ODN to a cross-linking agent. In method A, ODNs containing a highly nucleophilic terminal thiophosphate residue were reacted with haloacetamido deriva-

tive **11b**, **12b**, or **14**. The reactions were carried out in 50% aqueous DMF using 2–3-fold excess of the reagents. As we had noticed before,<sup>13</sup> this reaction produced a minor side product, identified as the conjugate lacking the characteristic long-wavelength absorbance (max1 in Table 1). Most likely this product resulted from competitive reaction of the cyclopropyl function with the terminal phosphorothioate residue. This was supported by the fact that no ODN-related side products were observed in the reaction using TFP ester type reagents and amino tailed ODNs (method B).

In method B, the alkylating residues were linked to 5'-alkylamine-modified ODNs via amide bonds. The amine-modified ODNs were first converted to the triethylammonium (TEA) salts by reverse phase HPLC. The TEA salts of ODNs as well as TFP esters are soluble in DMSO and allow the conjugation chemistry to be carried out under anhydrous conditions. After treatment with 5–20 equiv of the appropriate TFP ester (**18b**, **19b**, **22b**, or **23b**), the crude CPI-ODN conjugates were precipitated and purified by reverse phase HPLC to give the desired reagents in 35–78% yield.

The conjugates were routinely analyzed by nuclease digestion assay to monitor the nucleoside content as well as the presence of alkylating group. These preparation and analysis steps are shown in Figure 2 for a typical MCPI-ODN conjugate.

**Stability of CPI-ODN Conjugates.** We have previously shown that a conjugated CPI moiety is somewhat more labile than free CPI in mild acidic conditions. A conjugate which had been prepared by reaction of bromoacetamido CPI (**2**) with an ODN-bearing terminal thiophosphate had a half-life of about 3 h at pH 4.5 as measured by UV spectroscopy at 360 nm.<sup>13</sup> The conjugates synthesized in this work had similar stability (Table 2). Half-lives of tens of minutes were observed at a pH of 4 (22 °C) for the tethered CPI function. This is in contrast to the unconjugated **8** and **22c** (prepared by reacting **22b** with 3-aminopropanol), which were significantly more stable under these conditions. We assume that this enhanced lability (50–100 times) is due to an effect of the ODN. Conjugation of the CPI moiety to the ODN either might allow a proximity effect (proximity to nucleophilic DNA centers) or might involve acid catalysis by phosphate-coordinated Mg<sup>+2</sup> cations. At pH 4, phosphate-mediated acid catalysis may also be a factor. Whatever the mechanism is, CPI hydrolysis and/or alkylation of adjacent bases or phosphates (self-alkylation) are potential results of the activation.

The acid lability of ODN-conjugated CPI (MCPI) was not a problem at pH 7.2, where most of the conjugates used in this work did not show any significant decomposition over hours of incubation even at elevated temperature (37 °C). The rate of decomposition of alkylating function for the CPI- or MCPI-ODN conjugates is independent of the absolute configuration of the reactive center at either pH 4 or 7.2, indicating that hydrolysis and not ODN interaction is the main degradation pathway. This was supported by the fact that one major product was observed by HPLC. The CPI-DPI-ODN and MCPI-DPI-ODN conjugates, however, when incubated under the same conditions, gave multiple unidentified products. This observation supports a self-alkylation pathway for degradation of MCPI-DPI or CPI-DPI conjugates. Natural (+)-enantiomers were considerably more reactive than the unnatural ones. For example, the ODN-bearing (+)-CPI-DPI residue (also the most reactive DNA alkylating conjugate used in this work) was the least stable (half-life about 10 h at 37 °C in a neutral solution), while (–)-MCPI-DPI-ODN was the most stable with a half-life of more than 100 h. Double-stranded DNA structures could be involved in these cases. Although the oligonucleotide

**Table 1.** UV Properties of Some MCPI and CPI Compounds

compd	solvent	$\lambda$ max1 (nm)	$\epsilon$ max1 ( $M^{-1} cm^{-1}$ )	$\lambda$ max2 (nm)	$\epsilon$ max2 ( $M^{-1} cm^{-1}$ )	$\lambda$ max3 (nm)	$\epsilon$ max3 ( $M^{-1} cm^{-1}$ )	$\lambda$ min2 (nm)	$\epsilon$ min2 ( $M^{-1} cm^{-1}$ )	$\lambda$ min1 (nm)	$\epsilon$ min1 ( $M^{-1} cm^{-1}$ )
<b>8</b>	EtOH	342	13800	279	17400			248	1600	302	8000
<b>14</b>	MeOH	344	14200	283	14700			251	4000	302	8500
<b>12b</b>	MeOH	344	13300	284	15500			251	2500	303	7600
<b>11b</b>	MeOH/H <sub>2</sub> O	351	13600	289	14700			253	3200	305	7400
<b>18b</b>	MeOH	344	14000	283	14800			250	2800	302	8000
<b>19b</b>	MeOH	347	14000	283	17400			248	2700	312	8000
<b>22b</b>	MeCN	350	26000	312	22000	262	35100	291	18000	325	18700
<b>23b</b>	MeCN	349	26600	312	24200	262	37300	290	20700	325	19500

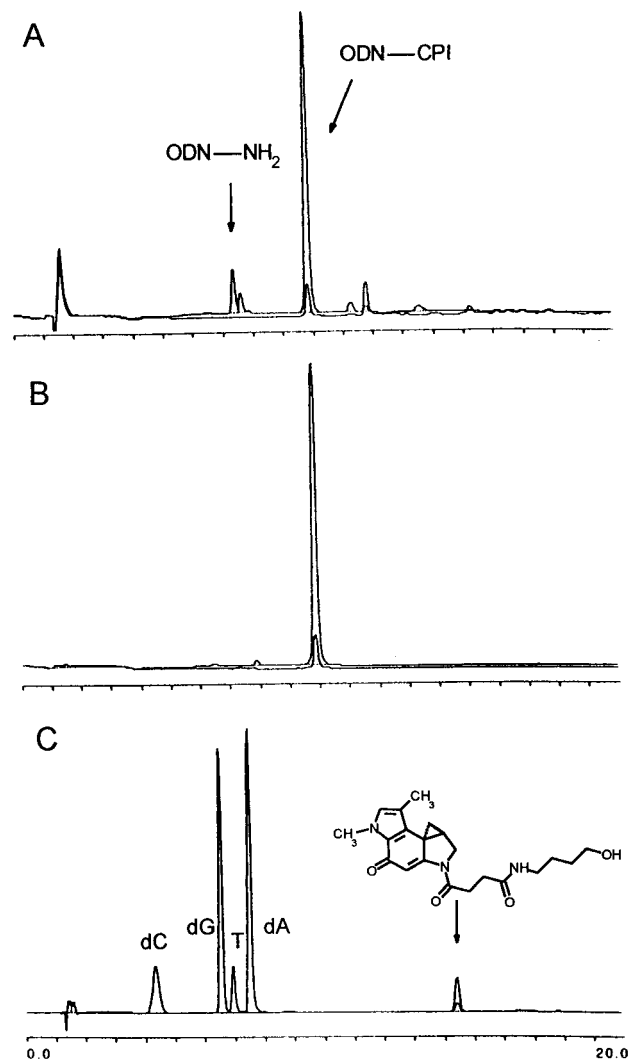


**Figure 2.** Analysis of a MCPI-ODN conjugate: (A) crude reaction mixture; (B) purified conjugate; (C) nuclease digest. The analytical reverse phase HPLC was performed on a Rainin C-18 column (4.5 × 150 mm) in a gradient of acetonitrile (0–60%) in 0.1 M triethylammonium acetate buffer (pH 7.5). Flow rate was 1 mL/min. Dual wavelength detection was used: fine line, 260 nm; bold line, 350 nm. sequence used in this study does not have any obvious self-complementarity, some nonperfect duplexes could be formed due to the increased ability of the dimeric agents to bind to and stabilize such duplexes.<sup>32–34</sup> This could lead to more rapid reaction for the one isomer and stabilization for the other.

**Reactivity and Site Specificity.** The site specificity of alkylation for CC-1065 and its analogues can be summarized

(32) Kim, D.-Y.; Swenson, D. H.; Cho, D.-Y.; Taylor, H. W.; Shih, D. S. *Antisense Res. Dev.* **1995**, *5*, 149–154.

(33) Kim, D.-Y.; Shih, D. S.; Cho, D.-Y.; Swenson, D. H. *Antisense Res. Dev.* **1995**, *5*, 49–57.

(34) Lukhtanov, E. A.; Kutuyavin, I. V.; Gamper, H. B.; Meyer, R. B., Jr. *Bioconjugate Chem.* **1995**, *6*, 418–426.

**Table 2.** Stability of ODN Conjugates

conjugate <sup>a</sup> or compd	pH 4.0 <sup>b</sup>		pH 7.2 <sup>c</sup>	
	$k_{obs} \times 10^4$ (s <sup>-1</sup> )	$t_{1/2}$ (min)	$k_{obs} \times 10^6$ (s <sup>-1</sup> )	$t_{1/2}$ (h)
(+)-CPI-DPI-ODN	8.5 ± 0.5	14	1.9 ± 0.3	10
(-)-CPI-DPI-ODN	7.2 ± 0.1	16	3.0 ± 0.2	63
(+)-MCPI-DPI-ODN	5.9 ± 0.1	20	4.0 ± 0.3	48
(-)-MCPI-DPI-ODN	4.4 ± 0.2	26	1.7 ± 0.4	> 115
(+)-CPI-ODN	2.6 ± 0.1	44	4.4 ± 0.3	44
(-)-CPI-ODN	3.1 ± 0.1	37	5.2 ± 0.2	37
(+)-MCPI-ODN	1.9 ± 0.1	60	3.4 ± 0.3	56
(-)-MCPI-ODN	2.0 ± 0.1	58	3.6 ± 0.3	53
<b>8</b>	0.054 ± 0.001	2148	<i>d</i>	
<b>22c</b>	0.091 ± 0.003	1275	<i>d</i>	

<sup>a</sup> The conjugates were prepared by reaction of TFP esters of corresponding alkylating agents with 5'-hexylamino tailed ODN (prepared using method B). <sup>b</sup> Determination of rates of acid catalyzed hydrolysis was carried out at 22 °C in an acidic buffer (pH 4). The buffer contained 8 mM citric acid and 4 mM Na<sub>2</sub>HPO<sub>4</sub> in 50% aqueous methanol. <sup>c</sup> The experiments were carried out in a buffer containing 140 mM KCl, 10 mM MgCl<sub>2</sub>, and 20 mM HEPES (pH 7.2) at 37 °C. <sup>d</sup> Reaction was too slow to measure accurately.

by three types of consensus sequences: PyNTTA\*, AAAAA\*, and T/AT/AA\*.<sup>23,24</sup> The effects of target site sequence on reaction rates, however, are less investigated.<sup>20,35</sup> The system described here offers an opportunity to evaluate the reactivity of CPI with any possible duplex site via direct positioning of the ODN-conjugated CPI into the target site.

Figure 3 shows the design of the ODN hairpin target we used to investigate the target sequence preference and effect of the tether to the ODN. The targets were designed with an invariable 5' single-stranded region, which was the complementary binding site for (+)- and (-)-CPI conjugates of the test dodecanucleotide ODN, and an adjacent variable, double-stranded hairpin segment for binding and reaction of the alkylating group. The sequences are listed in Table 3. Since the conjugated alkylating residue can, in principle, interact with adjacent hairpin duplex as well as fold back into the duplex formed by the ODN, the ODN sequence was made G-C rich, which is unfavorable for binding and alkylation by CPI. In addition, molecular modeling indicated that the fifth and sixth positions of the double-stranded region would be alkylated.

The alkylation rate was determined by monitoring the decrease in the characteristic long-wavelength band shown in Figure 4. A 2-fold excess of the target hairpin was used to insure complete duplexing of the reactive ODN. For determination of efficiency and site of alkylation, <sup>32</sup>P-labeled targets were treated with reactive ODN conjugate and incubated overnight (15 h) at 37 °C. The yield of alkylation was determined by denaturing polyacrylamide gel electrophoresis (PAGE) of the reaction; products of alkylation reactions have different mobilities from starting oligonucleotides. The sites of alkylation were determined by denaturing PAGE analyses of heat/piperidine-treated reactions.

(35) Boger, D. L.; Jonson, D. S.; Yun, W. *J. Am. Chem. Soc.* **1994**, *116*, 1635–1656.

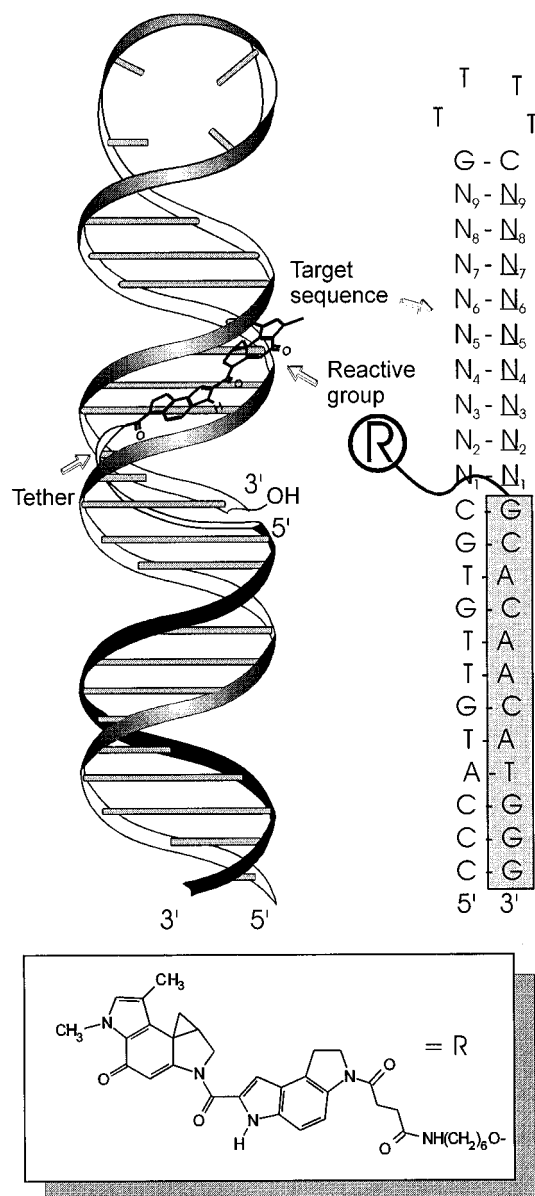


**Figure 3.** Diagram of target hairpin ODNs with bound MCPI-DPI-ODN conjugate. The structure of the linker for the MCPI-DPI-ODN conjugate is illustrated. Structures of the alkylation sites and the results of cross-linking reactions are shown in Table 3.

Table 3 summarizes the results for an ODN carrying natural (+)-MCPI-DPI, (+)-MCPI, and unnatural (–)-MCPI-DPI enantiomers. Even with this limited set of DNA targets, some general trends can be observed. The tethered (+)-MCPI-DPI can alkylate any accessible adenine residue, with the reaction rates varying with the target sequence and linker. When the linker allows movement of the alkylating group, conjugation does not change the known sequence preference characteristic for free CPI-DPI. For example, oligoadenylate sequence **I** proved to be a very good target, predominantly alkylated at the A<sub>6</sub> position, consistent with previous observation.<sup>13</sup> Other A–T-rich sequences such as 5'TTTAA (**III**), 5'TTTTA (**V**, **VI**), 5'TAAAA (**XI**), and 5'GTAAA (**XII**) also demonstrate good reactivity, in accord with previously established rules for free CPI.<sup>23,24</sup> An alternating AT sequence (**XVIII**) is less suitable as a target. Not surprisingly, **VIII** and **XVI**, with no adenine residues in the target site, show no reactivity.

It is important to note that no reaction was detected for target **XX**. In contrast to all targets tested, this 21 nucleotide ODN has a single-stranded A<sub>6</sub> target site. The lack of reactivity in

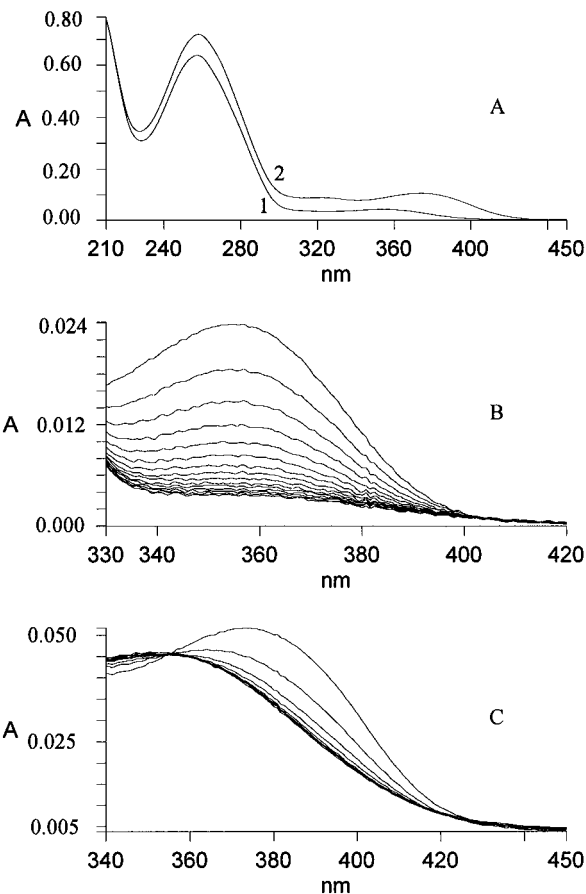


**Figure 4.** Kinetic determination from loss of CPI chromophore. (A) UV–visible spectra of 8  $\mu$ M MCPI-ODN (**1**) and 8  $\mu$ M MCPI-DPI-ODN (**2**) conjugates in 4 mM HEPES (pH 7.2). (B) Time course for the cross-linking reaction of the (+)-MCPI-ODN conjugate with the target ODN (**I**). The spectra were taken in a buffer containing 20 mM HEPES (pH 7.2) (37 °C) in 10 min intervals. (C) Time course for the cross-linking reaction of the (+)-MCPI-DPI-ODN conjugate with the target ODN (**I**). The spectra were taken in a buffer containing 20 mM HEPES (pH 7.2) (37 °C) in 2 min intervals.

this case supports the case for the minor groove-specific, hybridization-triggered nature of the reactions with a duplex target.

The importance of correct placement of the CPI in the targeted site can be seen when the 5'-TTTTAC sequence is placed at varying distances from the ODN-CPI conjugate. This sequence provides a good binding site for the (+)-MCPI-DPI and contains a single A for reaction. It is found in the four target ODNs **V–VIII**. The optimum reaction was observed when the alkylated adenine was in the sixth position from 5'-end of the target (**VI**). Shift of the binding site one base in the 5'-direction (**V**, closer to the bound ODN) results in slightly less reactivity. Shift of the target site away from the ODN binding site either significantly reduces (target **VII**) or completely diminishes the reaction (target **VIII**). Sequencing of the alkylation reactions confirms this stereospecificity: the most reactive targets (**I**, **III**, **VI**, and **XII**) all have an adenine in the sixth residue from the 5'-end of the hairpin, and all show reaction at that site.

The natural (+)-MCPI-DPI enantiomer is at least 10 times more reactive than the (–)-isomer, reflecting their similarity with CPI enantiomers. As suggested by Boger and co-workers,<sup>31,35,36</sup> the origin for the difference in efficiency of DNA alkylation arises from steric interaction between the C7 methyl group and the base adjacent to the alkylated adenine. This steric

(36) Boger, D. L.; Johnson, D. S.; Yun, W.; Tarby, C. *Bioorg. Med. Chem.* **1994**, *2*, 115–135.

**Table 3.** Efficiency and Position of Alkylation by Tethered (+)-MCPI-DPI, (-)-MCPI-DPI, and (+)-MCPI at Various DNA Sites

Sequence <sup>a</sup>	(+) -MCPI-DPI-ODN				(-) -MCPI-DPI-ODN				(+) -MCPI-ODN				
	$k_{\text{obs}} \times 10^3$ (s <sup>-1</sup> ) <sup>b</sup>	$t_{1/2}$ min	%	position of alkylation	$k_{\text{obs}} \times 10^4$ (s <sup>-1</sup> )	$t_{1/2}$ min	extent of alkn (%)	position of alkylation	$k_{\text{obs}} \times 10^3$ (s <sup>-1</sup> ) <sup>b</sup>	$t_{1/2}$ <sup>c</sup> min	extent of alkn (%) <sup>d</sup>	position of alkylation	
5'N <sub>1</sub> N <sub>2</sub> N <sub>3</sub> N <sub>4</sub> N <sub>5</sub> N <sub>6</sub> N <sub>7</sub> N <sub>8</sub> N <sub>9</sub> 3'TTTTTTCGC 5'	I	6.1 ± 0.3	2	100	A <sub>6</sub>	N/A	640	60	A <sub>2</sub>	0.41 ± 0.01	28	100 (80)	A <sub>5</sub>
5'ACAAACGCG 3' 3'TGTTTGC GC 5'	II	0.37 ± 0.01	31	95	A <sub>5</sub>	no reaction <sup>e</sup>	-	0	-	N/A	~400	75 (60)	A <sub>3,4</sub>
5'ATTTAAGCG 3' 3'TAAATTCGC 5'	III	4.0 ± 0.2	3	100	A <sub>6</sub>	1.9 ± 0.1	61	95	A <sub>3,4</sub>	N/A	~320	80 (75)	A <sub>5</sub>
5'TGTTATGCG 3' 3'ACAAACGCG 5'	IV	0.66 ± 0.01	17.5	100	A <sub>5</sub>	1.8 ± 0.2	64	75	A <sub>4</sub>	N/A	-	(20)	A <sub>5</sub>
5'TTTTACGCG 3' 3'AAAATGCGC 5'	V	0.88 ± 0.03	13	100	A <sub>5</sub>	2.7 ± 0.1	43	95	A <sub>3</sub>	N/A	~800	50 (45)	A <sub>5</sub>
5'GTTTACCG 3' 3'CAAAATGCG 5'	VI	1.9 ± 0.1	6	100	A <sub>6</sub>	2.7 ± 0.05	43	100	A <sub>4</sub>	no reaction <sup>f</sup>	-	(0)	-
5'GCTTTACG 3' 3'CGAAAATGC 5'	VII	0.075 ± 0.005	154	N/D	A <sub>7</sub>	5.0 ± 0.1	23	100	A <sub>5</sub>	no reaction <sup>f</sup>	-	(0)	-
5'GCGTTTAC 3' 3'CGCAAATG 5'	VIII	slow reaction	-	15	N/D	3.7 ± 0.1	31	100	A <sub>5</sub>	no reaction <sup>f</sup>	-	(0)	-
5'TTTACCGCG 3' 3'AAATGCGC 5'	IX	0.34 ± 0.01	34	100	A <sub>4</sub>	3.8 ± 0.1	30	100	A <sub>3</sub>	N/A	-	(15)	A <sub>4</sub>
5'TTACGCGCG 3' 3'AATGCGCGC 5'	X	0.025 ± 0.001	462	50	A <sub>3</sub>	slow reaction	-	~10	A <sub>1</sub>	N/A	-	(20)	A <sub>3</sub>
5'TAAAACGCG 3' 3'ATTTTGC GC 5'	XI	0.13 ± 0.01	9	100	A <sub>5</sub>	slow reaction	-	~20	A <sub>2</sub>	N/A	~400	70 (40)	A <sub>3,4,5</sub>
5'TGTAAAGCG 3' 3'ACATTCGC 5'	XII	4.2 ± 0.2	3	100	A <sub>5,6</sub>	slow reaction	-	10	N/D	N/A	~600	(40)	A <sub>4,5</sub>
5'GATTACGCG 3' 3'CTAATGCGC 5'	XIII	0.56 ± 0.02	21	100	A <sub>5</sub>	1.0 ± 0.1	115	85	A <sub>4</sub>	-	~280	75 (65)	A <sub>5</sub>
5'GATAACGCG 3' 3'CTATTGCGC 5'	XIV	1.1 ± 0.1	10.5	100	N/D	slow reaction	-	15	A <sub>3</sub>	N/A	~240	80 (70)	A <sub>3,5</sub>
5'GCACAAGCG 3' 3'CGTGTCGC 5'	XV	0.42 ± 0.01	27.5	100	N/D	no reaction <sup>e</sup>	-	0	-	no reaction <sup>f</sup>	-	(0)	-
5'TTTTGC GC 3' 3'AAAACGCGC 5'	XVI	no reaction <sup>e</sup>	-	0	-	1.5 ± 0.1	77	100	A <sub>3</sub>	no reaction <sup>f</sup>	-	(0)	-
5'AGTTATGCG 3' 3'TCAATACGC 5'	XVII	0.48 ± 0.01	24	100	A <sub>5</sub>	2.5 ± 0.1	46	95	A <sub>4</sub>	-	~800	50 (50)	A <sub>5</sub>
5'ATATATGCG3' 5'TATATACGC 5'	XVIII	0.19 ± 0.01	61	-	N/D	0.31 ± 0.02	343	-	N/D	no reaction <sup>f</sup>	-	(0)	-
5'TTTTTTGC GC 3' 5'AAAAAACGC 5'	XIX	no reaction <sup>e</sup>	-	0	-	7.5 ± 0.3	15.4	100	A <sub>5</sub>	no reaction <sup>f</sup>	-	(0)	-
5'AAAAAAGCG 3'	XX	no reaction <sup>f</sup>	-	0	-	no reaction <sup>f</sup>	-	0	-	no reaction <sup>f</sup>	-	(0)	-

<sup>a</sup> See Figure 3 for structure and numbering of hairpin targets. <sup>b</sup>  $K_{\text{obs}}$  was determined from loss of CPI chromophore (330–450 nm) as shown in Figure 4. <sup>c</sup> Half-lives of reactions with (+)-MCPI conjugate were determined as times required for absorbance at 355 nm to decrease by one-half. (Many of the reactions did not go to completion.) <sup>d</sup> Extent of alkylation by (+)-MCPI-ODN was determined after 15 h incubation by two different assays: by UV spectrometry as illustrated in Figure 4 (open numbers) or by gel-electrophoretic analysis of radiolabeled cross-link products (numbers in parentheses). <sup>e</sup> No change in the UV spectrum of the reaction mixture was observed after 3 h. <sup>f</sup> No reaction was observed by analysis of radiolabeled cross-link products after 15 h (37 °C).

interaction is more pronounced for the unnatural (-)-enantiomer. Introduction of the N5-methyl group, which protrudes away from the minor groove, does not affect the general distinction between (+)- and (-)-enantiomers but, as will be pointed out later, significantly decreases rate of DNA alkylation for both enantiomers. In addition, the observed difference (~10×) is substantially smaller than was reported for free (+)- and (-)-CPI-DPI (100–500×).<sup>29,36</sup>

Extended incubation of (+)-MCPI-DPI-ODN with targets usually resulted either in a quantitative reaction or in no reaction at all, depending on the sequence of the targets (Table 3). In contrast, (-)-MCPI-DPI-ODN frequently showed intermediate efficiency in the overnight reaction (20–95%), even when there was a reasonably high rate of alkylation ( $k = 1-3 \times 10^{-4}$

s<sup>-1</sup>). For example, a (+)-MCPI-DPI-ODN derivative slowly but quantitatively reacts with target **XV** ( $t_{1/2}$  of 27.5 min). The corresponding (-)-MCPI-DPI-ODN conjugate showed just two times slower reaction with another target **IV** ( $t_{1/2}$  of 64 min), but overnight incubation of this complex resulted in 75% yield of the cross-linking reaction. Having almost identical reactivity toward targets **III** and **IV** ( $t_{1/2}$  of 61 and 64 min, respectively), a (-)-MCPI-DPI-carrying ODN showed lower efficiency of alkylation (95 and 75%). The difference in the alkylation efficiencies could be explained by reversibility of the N3-adduct,<sup>37</sup> which could be more pronounced for the unnatural enantiomer.<sup>36</sup>

(37) Warpehoski, M. A.; Harper, D. E.; Mitchell, M. A.; Monroe, T. J. *Biochemistry* **1992**, *31*, 2502–2508.

The rate of alkylation by tethered (+)-MCPI was substantially less than both (+)-MCPI-DPI and (–)-MCPI-DPI. Except for the super reactive site **I**, alkylation by the monomeric agent was about 100 times slower than by (+)-MCPI-DPI or ~10 times slower than by (–)-MCPI-DPI (Table 3). Alkylation at the site **I** appears to be favored by the unusual bent structure of long A tracts,<sup>38</sup> thus diminishing the difference between the monomeric and dimeric agents.

No alkylation was observed when targeted adenines were placed six bases or farther into the adjacent duplex (sequences **VI**, **VII**, and **VIII**). These sequences were not used for comparison of reactivity since their adenines, apparently, are out of reach for the tethered (+)-MCPI residue.

The reversibility of alkylation by the monomeric (+)-MCPI was even more pronounced than for (–)-MCPI-DPI. After 15 h incubation (at 37 °C), most of the reactions involving the monomeric agent did not go to completion and reached plateaus (as followed by UV spectroscopy). Moreover, the efficiency of alkylation as measured by gel electrophoresis of the radio-labeled cross-link products was significantly lower than that measured by the UV method (Table 3). Decomposition of the N3-adenine adduct during electrophoresis, which was observed as a smear below the cross-link bands, may account for the difference. This is in accord with the known retroalkylation of the N3-adenine adduct,<sup>22</sup> which is highly dependent on the extent of noncovalent binding.<sup>37</sup>

**Non-Oligonucleotide-Specific (“Anchor”) Effects.** Since these ODNs are conjugated to strong minor groove binding agents such as simplified analogues<sup>34,35</sup> of CC-1065,<sup>32,33</sup> it is important to show that the observed alkylation is completely directed by ODN binding and not controlled by the minor groove binder (“anchor” effect). A noncomplementary ODN, CpCpCpApTpGpTpTpGpTpGpC, carrying a (+)-MCPI-DPI residue conjugated to its 3'-end was prepared and reacted with a target sequence (**I**). A small nonspecific reaction due to the anchor effect, with a half-life of approximately 6 h (37 °C), was seen. The same concentration (2 μM) of free (+)-MCPI-DPI (**22c**) alkylated the same target with a half-life of 7 min. The complementary ODN bearing the (+)-MCPI-DPI residue (Table 3) alkylated the target with a half-life of 2 min. Similar results were obtained with the other hairpin targets. These data demonstrate that the observed reactions (Table 3) are ODN-sequence dependent and not a result of an anchor effect, and that conjugation of the minor groove binding agent to the ODN significantly masks its inherent propensity to bind to A-T-rich sites in the minor groove. This is likely due to repulsion between the negatively charged backbones of target DNA and reactive ODN. The anchor effect was found to be negligible for (–)-MCPI-DPI, (+)- or (–)-MCPI, and (+)- or (–)-CPI conjugates, a reflection of their reduced minor groove binding affinity (data not shown).

**Binding Mode and Effect of Spacer Arm Structure.** An interesting feature of CPI compounds is that their orientation in the minor groove dictates which strand can be alkylated. Thus (+)-CC-1065 covers a four-base region within the minor groove in 5'-direction from the covalently modified adenosine. Conversely, the (–)-enantiomer of CC-1065 binds in the reverse orientation relative to the modified adenine. We found that the same rules apply to the tethered alkylators (Figure 5). If (+)-CPI is conjugated to the 5' end of the ODN, it would be expected to alkylate an adenine either in the complementary strand of the adjacent duplex region (mode 1) or in the carrier ODN if it folds back on itself (mode 2). However, unlike free CPI, which

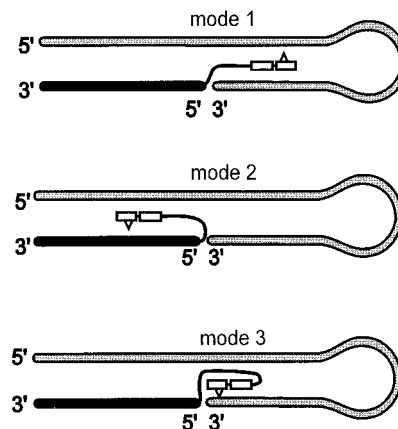


**Figure 5.** Possible cross-linking modes for the tethered (+)-CPI-DPI group.  $\Delta$  indicates positioning of the cyclopropane ring.

can slide along the minor groove or flip around to achieve alkylation of the opposite strand in the same DNA site, the conjugated CPI moiety is structurally constrained by tethering. This difference is very effectively demonstrated when alkylation of A<sub>6</sub>/T<sub>6</sub> DNA site is compared for free MCPI-DPI (**23c**) and the MCPI-DPI-ODN conjugates. This same sequence is presented in two target ODNs (sequences **I** and **XIX**, Table 3) with opposite positioning. Only target **I** was efficiently alkylated by the (+)-MCPI-DPI-ODN, while no reaction was observed for target **XIX** since it would require unfavorable mode 3 for alkylation (Figure 5). Unconjugated **23c**, on the other hand, reacted with both targets with approximately equal efficiency (data not shown). Similarly, tethered (–)-MCPI-DPI reacted efficiently with target **XIX** but not with target **I** in accordance with the opposite alkylation mode. However, in contrast to (+)-MCPI-DPI, a very slow contra strand alkylation ( $t_{1/2} > 600$  min) was observed for (–)-enantiomer (target sequences **I** and **XI**) despite the unfavorable orientation of the adenine stretch. This difference may lie in the strength of noncovalent minor groove binding. While (+)-dimer preferably binds very strongly to target **XIX** in mode 1, the (–)-enantiomer (being directed to target **I**) may bind more weakly and also accept an inverted binding mode (mode 3).

Another important feature of conjugated CPI is that it tends to occupy the most distal position to avoid looping out the spacer arm. The overall length of the conjugated CPI residue (including the spacer arm) determines the reachable range. For example, MCPI-DPI residue with the standard C6 linker has the highest alkylation rate when the target adenine in the TTTTAC site is in the sixth position relative to the attachment point (sequence **VI**, Table 3). Shifting the site further out results in almost complete loss of reactivity (sequence **VII**), while closer placement (sequence **V**) gives a significant drop in the reaction rate. Adjustment of the spacer arm length can fine tune the reactivity for target **V**. For instance, replacement of the C6 linker with a C4 linker provides a slight increase (~20%) in the reaction rate (data not shown).

Figure 6 shows the effect of the spacer arm structure on reactivity of the MCPI-ODN conjugates with target **I**. Generally, conjugates which have linker arms of 10–12 atoms in length (counting between the 5' terminal phosphorus atom and N2 nitrogen) have similar rates of reaction with the target. A reasonable degree of tether flexibility is apparently necessary for conjugated CPI to bind in the minor groove and attain the required conformation for alkylation. This can explain the low reactivity for two conjugates with short and rigid spacer arms. Structural features of the spacer arm such as hydrophobicity and hydrogen bonding amide groups are factors which could

(38) Crothers, D. M.; Haran, T. E.; Nadeau, J. G. *J. Biol. Chem.* **1990**, *265*, 7093–7096.



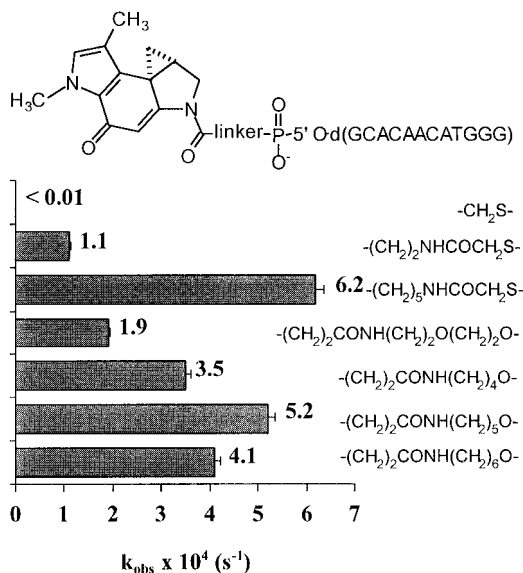


**Figure 6.** Effect of spacer arm structure on reactivity of (+)-MCPI-ODN conjugates. The 2  $\mu\text{M}$  conjugates were reacted with target ODN **I** (4  $\mu\text{M}$ ) at 37  $^{\circ}\text{C}$  in a buffer containing 140 mM KCl, 10 mM MgCl<sub>2</sub>, and 20 mM HEPES (pH 7.2). Kinetics were determined from loss of CPI chromophore.

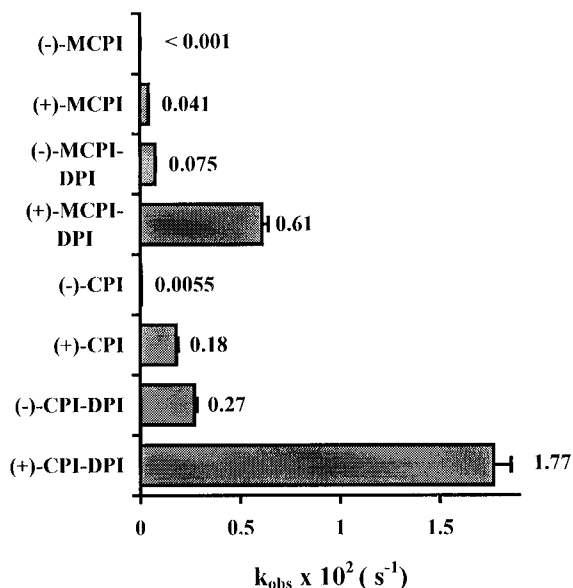


**Figure 7.** Relative reactivity of cross-linking ODNs. The conjugates (2  $\mu\text{M}$ ) were reacted either with target ODN **I** (4  $\mu\text{M}$ ) for (+)-enantiomers or with target **XIX** for (-)-enantiomers at 37  $^{\circ}\text{C}$  in a buffer containing 140 mM KCl, 10 mM MgCl<sub>2</sub>, and 20 mM HEPES (pH 7.2). Kinetics were determined from loss of CPI chromophore.

additionally contribute to the interaction with the minor groove and subsequently affect reactivity. The hydrophilic 2-(2-aminoethoxy)ethyl linker, for instance, gives a (+)-MCPI-ODN conjugate that reacted almost three times slower than the equal length but more hydrophobic aminopentyl linker.

**Relative Reactivity of CPI Reagents and Analogues.** Figure 7 shows a comparison of the reactivity of various CPI reagents using an A<sub>6</sub>/T<sub>6</sub> motif in the target. Among the tested sequences, this motif was shown to be the best target site for all CPI reagents. To allow each enantiomer to bind in an orientation preferred for reaction, sequence **I** was used for (+)-enantiomers and sequence **XIX** for (-)-enantiomers. The rate of reaction within the site should not be affected significantly by the length of the linker because any adenine residue could act as a target. Three factors affected the rate of reaction: (i)

addition of the DPI subunit results in 10–15-fold increase in reactivity for (+)-enantiomers (this difference becomes as large as 100 $\times$  for sequences other than **I** and **XIX** (Table 3)) and  $\sim$ 50-fold for (-)-enantiomers, (ii) all (+)-enantiomers react faster than the corresponding (-)-enantiomers by a factor of 10–20, and (iii) addition of the N5-methyl group to CPI decreases reactivity by a factor of 3–5. The reactivity of the tested conjugates was therefore (+)-CPI-DPI > (+)-MCPI-DPI > (-)-CPI-DPI > (+)-CPI > (-)-MCPI-DPI > (+)-MCPI  $\gg$  (-)-CPI > (-)-MCPI.

The rate of N3-adenine alkylation by CPI and analogues is affected by the noncovalent minor groove binding interaction and by the inherent electrophilic reactivity of the cyclopropyl function.<sup>31</sup> The electrophilic reactivity can be estimated for different analogues by the rates of acid-catalyzed solvolysis.<sup>29</sup> In addition, structural elements, such as a C7 substituent, may affect the DNA alkylating reactivity.<sup>39</sup> We were surprised, therefore, to find that the rate of DNA alkylation by CPI analogues was 3–5 times higher than for the corresponding methylated MCPI compounds. Both have similar acid hydrolysis rates (half-lives of 35.8 and 36.7 h, respectively, at pH 4) and the same C7 substituent. Computer modeling indicates that the N5-methyl group is situated on the outer periphery of the agent and should not interfere with the interaction with minor groove binding. The difference may lie in hindrance to catalysis by phosphate-bound magnesium, as discussed above, or in the manner in which the agent's conformation is affected by DNA binding.

This new class of cross-linking oligonucleotides has promise in the research and diagnostic areas as a tool for DNA site specific modification and cleavage and in the therapeutic area as inhibitors of gene expression. The remarkable stability of the CPI-alkylating function in physiological buffer allows the reactive ODN to reach a DNA target while avoiding side reactions with cellular nucleophiles, after which the unique hybridization-triggered mechanism of activation provides a rapid and efficient cross-link with that target. The target site of the CPI moiety can be specified by the oligonucleotide, not by the much more restricted binding mode of CC-1065. The efficiency and rate of the reaction will depend somewhat on favorable binding sites for the tethered CPI, but the number of DNA sites suitable for conjugated CPI residue are significantly increased over CC-1065. The general requirement is that the site has to be three-to-four A-T base pairs long. The linker to the oligonucleotide limits freedom of alkylating CPI such that the targeted adenine has to be in the fifth or sixth position from the end of the ODN carrier. The reaction preference differences between the natural (+) and the unnatural (-)-enantiomers offers the advantage of targeting one DNA strand or the other. Structural modifications such as the introduction of the DPI binding subunit or N5-methylation allows for modulation of the reactivity. These same conjugates might also alkylate double-stranded DNA, either as part of a classical triple-stranded complex<sup>40</sup> or, as we have recently shown, in a recombinase-stabilized synaptic joint.<sup>41</sup>

## Experimental Section

**(1S)-3-(6-(N-(tert-Butyloxycarbonyl)amino)hexanoyl)-1-(chloromethyl)-6,8-dimethyl-1,2-dihydro-3H-pyrrolo[3,2-e]indol-5-ol ((1S)-9a).** To a solution of freshly prepared (1S)-7b (0.28 mmol) in 3.5 mL of dry DMA were added 6-(N-BOC-amino)hexanoic acid

(39) Asai, A.; Nagamura, S.; Saito, H. *J. Am. Chem. Soc.* **1994**, *116*, 4171–4177.

(40) Helene, C. *Anti-Cancer Drug Des.* **1991**, *6*, 569–584.

(41) Podyminogin, M. A.; Meyer, R. B.; Gamper, H. B. *Biochemistry* **1995**, *34*, 13098–13108.

(110 mg, 0.48 mmol) and EDC (300 mg, 1.56 mmol). After being stirred for 30 min, the mixture was cooled in ice and water (15 mL) was added. The resulting solid was collected by filtration, washed with water, and dried *in vacuo*. The crude product was purified by flash chromatography CH<sub>2</sub>Cl<sub>2</sub>–MeOH (20:1) to give (1S)-**9a** as an off-white solid after evaporation of the solvent (95 mg, 73%): <sup>1</sup>H NMR (CDCl<sub>3</sub>) δ 8.96 (br s, 1H), 8.04 (s, 1H), 6.73 (s, 1H), 4.54 (br s, 1H), 4.28 (d, 1H, *J* = 11 Hz), 4.13 (t, 1H, *J* = 8 Hz), 4.02 (s, 3H), 3.93 (m, 1H), 3.84 (m, 1H), 3.31 (t, 1H, *J* = 11 Hz), 3.15 (m, 2H), 2.7–2.4 (m, 2H), 2.37 (s, 3H), 1.83 (m, 2H), 1.7–1.4 (m, 4H overlapping with H<sub>2</sub>O and BOC), 1.43 (s, 9H). Anal. Calcd for C<sub>24</sub>H<sub>34</sub>N<sub>3</sub>O<sub>4</sub>Cl·0.3H<sub>2</sub>O: C, 61.41; H, 7.43; N, 8.95. Found: C, 61.66; H, 7.30; N, 8.61.

**(1S)-3-(3-(*N*-*tert*-Butyloxycarbonyl)amino)propanoyl)-1-(chloromethyl)-6,8-dimethyl-1,2-dihydro-3H-pyrrolo[3,2-*e*]indol-5-ol ((1S)-**10a**).** Compound (1S)-**10a** was synthesized by analogy with (1S)-**9a** using 3-(*N*-BOC-amino)propanoic acid in 83% yield: <sup>1</sup>H NMR (CDCl<sub>3</sub>) δ 8.69 (br s, 1H), 7.99 (s, 1H), 6.74 (s, 1H), 5.53 (br s, 1H), 4.25 (d, 1H, *J* = 11 Hz), 4.11 (t, 1H, *J* = 8 Hz), 4.02 (s, 3H), 3.93 (m, 1H), 3.85 (m, 1H), 3.60 (m, 2H), 3.33 (t, 1H, *J* = 11 Hz), 3.0–2.6 (m, 2H), 2.37 (s, 3H), 1.42 (s, 9H). Anal. Calcd for C<sub>21</sub>H<sub>28</sub>N<sub>3</sub>O<sub>4</sub>Cl: C, 59.78; H, 6.69; N, 9.96. Found: C, 59.88; H, 6.59; N, 9.56.

**(8aS)-2-6-(*N*-(Bromoacetyl)amino)hexanoyl)-1,2,8,8a-tetrahydro-5,7-dimethylcyclopropa[*c*]pyrrolo[3,2-*e*]indol-4-one ((8aS)-**11b**).** (1S)-**9a** (80 mg, 0.17 mmol) was suspended in 3 mL of ethyl acetate saturated with HCl. The suspension was stirred for 30 min and concentrated *in vacuo*. Residual HCl was removed by coevaporation with CH<sub>2</sub>Cl<sub>2</sub> (2 × 10 mL). The resulting hydrochloride (1S)-**9b** was dissolved in a mixture of acetonitrile (10 mL), triethylamine (3 mL), and water (3 mL). After 40 min, the solution was concentrated *in vacuo* to give an oil. This was dried by coevaporation with acetonitrile (3 × 10 mL) to give (8aS)-**11a** as a tan solid (95% pure by analytical reverse phase HPLC). To a suspension of the amine (8aS)-**11a** in 2 mL of DMF were added triethylamine (50 mL) and bromoacetic acid *N*-hydroxysuccinimide ester (50 mg, 0.21 mmol). After 30 min, the reaction mixture was partitioned between water and CH<sub>2</sub>Cl<sub>2</sub>. The water layer was separated and reextracted. The combined organic layer was washed with 5% NaHCO<sub>3</sub>, dried over Na<sub>2</sub>SO<sub>4</sub>, and concentrated *in vacuo*. Chromatography on silica gel, eluting with 5% MeOH–CH<sub>2</sub>Cl<sub>2</sub>, afforded 52 mg (68%) of (8aS)-**11b** as an off-white crystalline solid: <sup>1</sup>H NMR (CDCl<sub>3</sub>) δ 6.66 (br s, 1H), 6.57 (s, 1H), 4.3–3.8 (m, 7H), 3.35 (m, 2H), 2.85 (m, 1H), 2.52 (m, 2H), 1.98 (s, 3H), 1.92 (m, 1H), 1.73 (m, 2H), 1.59 (m, 2H), 1.43 (m, 2H), 1.16 (t, 1H, *J* = 5 Hz). Anal. Calcd for C<sub>21</sub>H<sub>26</sub>N<sub>3</sub>O<sub>3</sub>Br: C, 56.26; H, 5.85; N, 9.37. Found: C, 56.55; H, 6.02; N, 9.45.

**(8aS)-2-3-(*N*-(Bromoacetyl)amino)propanoyl)-1,2,8,8a-tetrahydro-5,7-dimethylcyclopropa[*c*]pyrrolo[3,2-*e*]indol-4-one ((8aS)-**12b**).** (8aS)-**12b** was synthesized by analogy with (8aS)-**11b** in 62% yield: <sup>1</sup>H NMR (CDCl<sub>3</sub>) δ 7.2 (br s, 1H), 6.58 (s, 1H), 4.3–3.8 (m, 7H), 3.65 (m, 2H), 2.88 (m, 1H), 2.72 (m, 2H), 1.98 (s, 3H), 1.92 (m, 1H), 1.18 (m, 1H). Anal. Calcd for C<sub>18</sub>H<sub>20</sub>N<sub>3</sub>O<sub>3</sub>Br: C, 53.21; H, 4.96; N, 10.34. Found: C, 53.41; H, 5.01; N, 10.57.

**(8aS)-2-(Chloroacetyl)-1,2,8,8a-tetrahydro-5,7-dimethylcyclopropa[*c*]pyrrolo[3,2-*e*]indol-4-one ((8aS)-**14**).** To a solution of freshly prepared (1S)-**7b** (0.28 mmol) in 3.5 mL of dry DMA were added bromoacetic acid (100 mg, 0.72 mmol) and EDC (300 mg, 1.56 mmol). After being stirred for 30 min, the solution was diluted with 10 mL of acetonitrile. Triethylamine (3 mL) and water (3 mL) were added to convert chloromethyl intermediate (1S)-**13b** into cyclic compound (8aS)-**14**. After 1 h, acetonitrile was removed on a rotary evaporator. The residual solution (~6 mL) was diluted with 15 mL of brine and extracted with dichloromethane (2 × 15 mL). The organic phase was washed with 5% NaHCO<sub>3</sub> (15 mL) and dried over Na<sub>2</sub>SO<sub>4</sub>. Purification by flash chromatography (CH<sub>2</sub>Cl<sub>2</sub>–MeOH, 20:1) gave (8aS)-**14** as an off-white solid (21 mg, 22%): <sup>1</sup>H NMR (CDCl<sub>3</sub>) δ 6.59 (s, 1H), 4.4–4.0 (m, 4H), 3.98 (s, 3H), 2.87 (m, 1H), 1.98 (s, 3H), 1.95 (m, 1H, partially overlapping with CH<sub>3</sub> singlet), 1.23 (t, 1H, *J* = 5 Hz). Anal. Calcd for C<sub>15</sub>H<sub>15</sub>N<sub>2</sub>O<sub>2</sub>Cl: C, 61.97; H, 5.20; N, 9.64. Found: C, 61.67; H, 5.14; N, 9.46.

**(8aS)-2,3,5,6-Tetrafluorophenyl 1,2,8,8a-tetrahydro-5,7-dimethyl-4-oxo-cyclopropa[*c*]pyrrolo[3,2-*e*]indole-2-succinate ((8aS)-**18b**).** To a suspension of freshly prepared (1S)-**7b** (0.9 mmol) in a mixture of dry CH<sub>2</sub>Cl<sub>2</sub> (7 mL) and MeOH (7 mL) were added succinic anhydride

(200 mg, 2 mmol) and triethylamine (0.5 mL, 3.65 mmol), and the resulting solution was stirred for 3 h. The solvents were removed by evaporation, and the crude product was purified by flash chromatography (CH<sub>2</sub>Cl<sub>2</sub>–MeOH–triethylamine, 90:10:2) to give the desired succinate (1S)-**16** as a tan solid foam (200 mg, 50%). It was dissolved in a mixture of acetonitrile (10 mL), triethylamine (3 mL), and water (3 mL). After being stirred for 45 min, the mixture was concentrated *in vacuo*. Residual water was removed by coevaporation with acetonitrile (3 × 10 mL). The resulting cyclic product (8aS)-**18a** (tan oil) was taken to the next step without additional purification. To a solution of the crude succinate ((8aS)-**18a**) in 5 mL of dry CH<sub>2</sub>Cl<sub>2</sub> were added dropwise triethylamine (200 mL) and 2,3,5,6-tetrafluorophenyl trifluoroacetate<sup>27</sup> (200 mL, 1.14 mmol). After being stirred for 1 h, the solution was concentrated *in vacuo*. Flash chromatography (3.5 × 15 cm, 40% ethyl acetate–hexane) afforded (8aS)-**18b** (180 mg) as a white crystalline solid (150 mg, 74% from (8aS)-**18a**): mp 158–160 °C (hexane/ethyl acetate): <sup>1</sup>H NMR (CDCl<sub>3</sub>) δ 7.00 (m, 1H), 6.58 (s, 1H), 4.4–4.1 (m, 1H), 3.99 (s with overlapping m, 4H), 3.3–2.7 (m, 5H), 1.98 (s, 3H), 1.92 (m, 1H), 1.22 (t, 1H, *J* = 4.5 Hz). Anal. Calcd for C<sub>23</sub>H<sub>18</sub>N<sub>2</sub>O<sub>4</sub>F<sub>4</sub>: C, 59.74; H, 3.92; N, 6.06. Found: C, 59.51; H, 3.72; N, 5.92. [α]<sub>D</sub><sup>25</sup>: +112° (c 0.005, CDCl<sub>3</sub>). (8*R*)-**18b** was prepared analogously from (1*R*)-**7b**: [α]<sub>D</sub><sup>25</sup>: –115° (c 0.004, CDCl<sub>3</sub>).

**(8aS)-2,3,5,6-Tetrafluorophenyl 1,2,8,8a-tetrahydro-7-methyl-4-oxo-cyclopropa[*c*]pyrrolo[3,2-*e*]indole-2-succinate ((8aS)-**19b**).** It was prepared by analogy with (8aS)-**18b** by starting from (1S)-3-(*tert*-butyloxycarbonyl)-1-(chloromethyl)-5-hydroxy-8-methyl-1,2-dihydro-3H-pyrrolo[3,2-*e*]indole ((1S)-**15a**)<sup>16,24,26</sup> in 44% yield: <sup>1</sup>H NMR (CDCl<sub>3</sub>) δ 9.61 (br s, 1H), 7.00 (m, 1H), 6.85 (s, 1H), 4.4–3.9 (m, 2H), 3.3–2.8 (m, 5H), 2.03 (s, 3H), 1.99 (m, 1H), 1.27 (m, 1H). Anal. Calcd for C<sub>22</sub>H<sub>16</sub>N<sub>2</sub>O<sub>4</sub>F<sub>4</sub>: C, 58.93; H, 3.60; N, 6.25. Found: C, 58.61; H, 3.78; N, 5.98. (8*R*)-**19b** was prepared analogously from (1*R*)-**15a**.

**(1S)-**20a**.** To a solution of freshly prepared (1S)-**7b** (0.33 mmol) in 5 mL of dry DMA were added 3-(*tert*-butyloxycarbonyl)-1,2-dihydro-3H-pyrrolo[3,2-*e*]indole-7-carboxylic acid<sup>28</sup> (100 mg, 0.33 mmol) and EDC (120 mg, 0.63 mmol). After being stirred for 5 h, the mixture was cooled in ice and water (15 mL) was added. The resulting solid was collected by filtration, washed with 1 M potassium phosphate and water, and dried *in vacuo* affording (1S)-**20a** as a green-yellow solid (161 mg, 91%). This was 95% pure by reverse phase HPLC. An analytical sample was purified by flash chromatography (5% MeOH in CH<sub>2</sub>Cl<sub>2</sub>): <sup>1</sup>H NMR (DMSO-*d*<sub>6</sub>) δ 11.62 (s, 1H), 9.79 (s, 1H), 7.8 (br s, 1H), 7.61 (br s, 1H), 7.31 (d, 1H, *J* = 9 Hz), 6.96 (br s, 2H), 4.63 (t, 1H, *J* = 10 Hz), 4.50 (d, 1H, *J* = 11 Hz), 4.1–3.8 (m with overlapping singlet (CH<sub>3</sub>) at 3.92 ppm, 6H), 3.55 (t, 1H, 10 Hz), 3.4–3.1 (m, 3H overlapping with the water peak), 2.31 (s, 3H), 1.51 (s, 9H). Anal. Calcd for C<sub>29</sub>H<sub>31</sub>N<sub>4</sub>O<sub>4</sub>Cl: C, 65.10; H, 5.84; N, 10.47. Found: C, 64.86; H, 5.94; N, 10.26. (1*R*)-**20a** was prepared analogously from (1*R*)-**7b**.

**(1S)-**21a**.** It was prepared by analogy with (1S)-**20a** starting from (1S)-3-(*tert*-butyloxycarbonyl)-1-(chloromethyl)-5-hydroxy-8-methyl-1,2-dihydro-3H-pyrrolo[3,2-*e*]indole ((1S)-**15a**) and 3-(*tert*-butyloxycarbonyl)-1,2-dihydro-3H-pyrrolo[3,2-*e*]indole-7-carboxylic acid. Crude (1S)-**21a** was purified by flash chromatography in ethyl acetate to give the title compound as a yellow-green solid (70% yield): <sup>1</sup>H NMR (DMSO-*d*<sub>6</sub>) δ 11.63 (s, 1H), 10.72 (s, 1H), 9.77 (s, 1H), 7.82 (m, 1H), 7.61 (m, 1H), 7.31 (d, 1H, *J* = 9 Hz), 7.04 (s, 1H), 6.96 (s, 1H), 4.65 (t, 1H, *J* = 10 Hz), 4.52 (d, 1H, *J* = 11 Hz), 4.02 (t, 2H, *J* = 8.5 Hz), 3.91 (d, 1H, *J* = 8.5 Hz), 3.58 (t, 1H, 9 Hz), 3.4–3.1 (m, 3H overlapping with the water peak), 2.35 (s, 3H), 1.52 (s, 9H). Anal. Calcd for C<sub>28</sub>H<sub>29</sub>N<sub>4</sub>O<sub>4</sub>Cl: C, 64.55; H, 5.61; N, 10.75. Found: C, 64.33; H, 5.73; N, 10.46. (1*R*)-**21a** was prepared analogously from (1*R*)-**15a** and 3-(*tert*-butyloxycarbonyl)-1,2-dihydro-3H-pyrrolo[3,2-*e*]indole-7-carboxylic acid.

**(8aS)-**22b**.** (1S)-**20a** (150 mg, 0.28 mmol) was suspended in 5 mL of ethyl acetate saturated with HCl. The suspension was stirred for 40 min and concentrated *in vacuo*. Residual HCl was removed by coevaporation with CH<sub>2</sub>Cl<sub>2</sub> (2 × 10 mL). The resulting orange solid ((1S)-**20b**) was dissolved in 1 mL of dry DMA. Succinic anhydride (30 mg, 0.3 mmol) and triethylamine (50 mL, 0.36 mmol) were added to produce succinate (1S)-**20c**. After being stirred for 3 h, the reaction mixture was diluted with acetonitrile (10 mL) followed by the addition

of triethylamine (3 mL) and water (3 mL) to effect cyclization. After 1 h, the volatiles were removed *in vacuo*, and to the residue (DMA ~1 mL) was added ether (20 mL) to precipitate the product (8aS)-**22a**. It was collected by filtration and dried *in vacuo* affording the succinate as a grey-yellow solid. To a suspension of (8aS)-**22a** in 3 mL of DMA were added triethylamine (200  $\mu$ L, 1.44 mmol) and 2,3,5,6-tetrafluorophenyl trifluoroacetate (140  $\mu$ L, 0.8 mmol). After being stirred for 1 h, the reaction mixture was added dropwise to 10 mL of 0.3 M potassium phosphate buffer (pH 7.5), the resulting precipitate was collected by filtration and washed with water (15 mL) and ether (5 mL). Drying *in vacuo* afforded (8aS)-**22b** as a yellow-green solid (138 mg, 72%):  $^1\text{H NMR}$  (DMSO- $d_6$ )  $\delta$  11.81 (s, 1H), 8.21 (d, 1H,  $J = 9$  Hz), 7.94 (m, 1H), 7.31 (d, 1H,  $J = 9$  Hz), 7.08 (s, 1H), 6.88 (s, 1H), 6.65 (s, 1H), 4.6–4.4 (m, 2H), 4.24 (t, 2H,  $J = 8$  Hz), 3.87 (s, 3H), 3.3 (m, 2H, overlapping with water), 3.18 (m, 1H), 3.06 (m, 2H), 2.91 (m, 2H), 1.97 (s, 3H), 1.92 (m, 1H, overlapping with  $\text{CH}_3$ ), 1.38 (m, 1H). Anal. Calcd for  $\text{C}_{34}\text{H}_{26}\text{N}_4\text{O}_5\text{F}_4 \cdot 2\text{H}_2\text{O}$ : C, 59.82; H, 4.43; N, 8.21. Found: C, 59.80; H, 4.04; N, 8.07. (8aR)-**22b** was prepared analogously from (1R)-**20a**.

**(8aS)-23b.** It was prepared by analogy with (8aS)-**22b** starting from (1S)-**21a** in 70% yield:  $^1\text{H NMR}$  (DMSO- $d_6$ )  $\delta$  11.83 (s, 1H), 11.55 (s, 1H), 8.22 (d, 1H,  $J = 9$  Hz), 7.94 (m, 1H), 7.31 (d, 1H,  $J = 9$  Hz), 7.09 (s, 1H), 6.89 (s, 1H), 6.69 (s, 1H), 4.7–4.3 (m, 2H), 4.25 (t, 2H,  $J = 8$  Hz), 3.3 (m, 2H, overlapping with water), 3.18 (m, 1H), 3.06 (m, 2H), 2.91 (m, 2H), 2.00 (s, 3H), 1.97 (m, 1H, overlapping with  $\text{CH}_3$ ), 1.40 (m, 1H). Anal. Calcd for  $\text{C}_{33}\text{H}_{24}\text{N}_4\text{O}_5\text{F}_4 \cdot 1.5\text{H}_2\text{O}$ : C, 60.09; H, 4.13; N, 8.49. Found: C, 60.29; H, 4.07; N, 8.29. (8aR)-**23b** was prepared analogously from (1R)-**21a**.

**Oligonucleotide Synthesis.** Oligonucleotides were synthesized on an Applied Biosystems Model 394 DNA synthesizer utilizing the 1  $\mu$ mol coupling program supplied by the manufacturer. 5'-Aminolinkers were introduced into ODNs on the DNA synthesizer using the appropriate phosphoramidite reagent. Phosphoramidites for introduction of 6-aminoethyl or 2-(2-aminoethoxy)ethyl residues were purchased from Glen Research (Sterling, VA). 5-(*N*-(Monomethoxytrityl)amino)pentyl and 4-(*N*-(monomethoxytrityl)amino)butyl (2-cyanoethyl)diisopropyl phosphoramidites were prepared as described by Connolly<sup>42</sup> for similar 3-aminopropyl compound. Oligonucleotides with terminal 3'- or 5'-thiophosphate group were synthesized using Chemical Phosphorylation Reagent from Glen Research (Sterling, VA) and 3H-1,2-benzodithiol-3-one 1,1-dioxide as the sulfurizing agent.<sup>43</sup> After ammonia deprotection, the ODNs were HPLC purified, detritylated, and precipitated from butanol as described previously.<sup>44</sup>

**Conjugation Method A. CPI-ODN Conjugates with a Thiophosphate Linkage.** To a solution of an ODN with a terminal thiophosphate (~0.25  $\mu$ mol) in 20  $\mu$ L of water were added triethylamine (0.5  $\mu$ L) and haloacetamido reagent (**11b**, **12b** or **14**) (20  $\mu$ L of a 33 mM solution in DMF, 0.66  $\mu$ mol). The progress of the reaction was monitored by analytical reverse phase HPLC on a Rainin C-18 column (4.5  $\times$  150 mm) in a gradient of acetonitrile (0–60%) in 0.1 M triethylammonium acetate buffer (pH 7.5). After 2 h, the solution was diluted with 0.8 mL of water and loaded onto a semipreparative reverse phase HPLC column (Polymer Labs, PLRP-S, 250  $\times$  4.6 mm). The conjugates were resolved as cleanly separated peaks using a linear gradient of 0–60% acetonitrile in 0.1 M sodium perchlorate (pH 7) over 20 min (flow rate = 2 mL/min). The desired fraction was taken to dryness on a Savant SpeedVac and reconstituted in 50  $\mu$ L of water. Acetone (1.5 mL) was added to precipitate the product while leaving the excess sodium perchlorate in solution. After centrifugation, the pellet was additionally washed with acetone and dried *in vacuo*. After reconstitution in ~0.1 mL of 10 mM HEPES (pH 7.2), the concentration was determined from the UV absorbance using  $1 A_{260} = 30 \mu\text{g/mL}$ .<sup>45</sup> Typical yield was 60–70% (from starting ODN).

**Conjugation Method B. ODN-CPI Conjugates with an Amide Linkage.** 5'-Alkylamine-modified ODN was synthesized and purified

by reverse phase HPLC using standard procedures.<sup>44</sup> After detritylation, the dried ODN was taken up in 0.5 mL of water and repurified on a Hamilton PRP-1 column (305  $\times$  7.0 mm) using a linear gradient of 0–40% acetonitrile in 0.1 M triethylammonium bicarbonate (pH 7) over 20 min (flow rate = 3 mL/min). The desired fraction was taken to dryness on a Savant SpeedVac and reconstituted in 0.5 mL of water. The concentration was determined from the UV absorbance at 260 nm. An aliquot of this stock solution containing ~0.25 mg of the ODN was dried in a 1.7 mL Eppendorf tube (Savant SpeedVac), then dissolved in 100  $\mu$ L of dry DMSO (Aldrich). Ethyldiisopropylamine (5  $\mu$ L) and 50  $\mu$ L (0.5 mg, 1.1  $\mu$ mol) of a 10 mg/mL solution of **18b**, **19b**, **22b**, or **23b** in DMSO were added, and the solution was kept at ambient temperature for 16 h. The crude ODN product was precipitated by adding the reaction mix to 2 mL of 2% sodium perchlorate in acetone. After centrifugation, the pellet was dried, dissolved in 0.5 mL of water, and purified by HPLC as described in method A. Yields varied from 35 to 78% (from starting ODN). Analytical preparation is shown in Figure 2. The conjugates were at least 90% pure by C18 analytical HPLC.

**Nuclease Digestion Analysis.** To a solution of CPI-ODN (~15  $\mu$ g) in 50  $\mu$ L of a buffer containing 50 mM Tris-HCl (pH 8.5) and 10 mM  $\text{MgCl}_2$  were added RQ1 DNase (5  $\mu$ L, 1000 U/mL), phosphodiesterase I (5  $\mu$ L, 100 U/mL), and calf intestine alkaline phosphatase (1  $\mu$ L, 650 U/mL). The solution was incubated at 37  $^\circ\text{C}$  for 30 h. Aliquots (10  $\mu$ L) were taken during this period to monitor the progress of the reaction by reversed phase HPLC in a gradient of acetonitrile 0–60% (50 mM triethylammonium acetate, pH 7.5) using a Rainin C18 (4.5  $\times$  150 mm) column. Waters 994 photodiode array detector was used to identify products of digestion by their UV spectra.

**Determination of Stability of ODN Conjugates in Physiological Buffer.** A 100  $\mu$ M solution of ODN conjugated with one of the alkylating agents was incubated at 37  $^\circ\text{C}$  in a buffer containing 140 mM KCl, 20 mM HEPES (pH 7.2), and 10 mM  $\text{MgCl}_2$ . As an internal unreactive standard, 100  $\mu$ M of a modified scrambled 12-mer ODN was added. The ODN had a CDPI<sub>2</sub> (3-carbamoyl-3H-pyrrolo[3,2-*e*]indole-7-carboxamide dimer) residue attached at the 3'-end as previously described.<sup>34</sup> To monitor the progress of the reaction, 10  $\mu$ L aliquots were taken every 15–24 h and analyzed by reverse phase HPLC in a gradient of acetonitrile 0–60% (50 mM triethylammonium acetate, pH 7.5) in 20 min using a Rainin C18 (4.6  $\times$  150 mm) column with a flow rate of 1 mL/min. The extent of degradation was measured as loss of the starting CPI-ODNs relative to the internal unreactive standard. This internal standard had a retention time longer than CPI-ODNs and did not interfere with measurement of starting material or degradation products. Pseudo-first-order rate constants were calculated from linear plots of  $\log(C/C_0)$  versus time. At least five time points were used for the calculation during at least 2 half-lives. The experiments were done in duplicate.

**Determination of Reaction Rates of DNA Alkylation and Acid-Catalyzed Solvolysis.** Determination of the reaction rate of cross-linking between the CPI-ODN conjugate and hairpin target was based on monitoring of long wavelength band as illustrated in Figure 4. The experiments were carried out in a buffer containing 140 mM KCl, 10 mM  $\text{MgCl}_2$ , and 20 mM HEPES (pH 7.2) at 37  $^\circ\text{C}$  using a Lambda 2 (Perkin-Elmer) spectrophotometer equipped with a PT-6 automatic temperature controller. Preheated at 37  $^\circ\text{C}$ , solutions of a CPI-ODN conjugate and a hairpin target were mixed in a UV cuvette to final concentration of 2 and 4  $\mu$ M, respectively. UV spectra (340–450 nm) were recorded periodically until no further change was detected in the spectra. Residual absorbance at the long-wavelength region (355 nm for MCPI-ODN and 375 nm for MCPI-DPI-ODN conjugates) was subtracted from the measured absorbances. Pseudo-first-order rate constants were calculated from linear plots of  $\log(A/A_0)$  versus time using at least eight time points spanning more than 2 half-lives. The error ranges (Table 3) represent maximal deviations from the calculated rate constants. Some of the experiments were performed in triplicate in order to ensure reproducibility. Variation did not exceed 5%.

Determination of rates of acid-catalyzed hydrolysis was carried out analogously at 22  $^\circ\text{C}$  in an acidic buffer (pH 4). The buffer contained 8 mM citric acid, and 4 mM  $\text{Na}_2\text{HPO}_4$  in 50% aqueous methanol. (Note: It was recently specified<sup>17</sup> that this mixture has a pH of 4 not 3 as earlier reported.<sup>16</sup>) The UV spectra were recorded every 5 min

(42) Connolly, B. A. *Nucleic Acids Res.* **1987**, *15*, 3131–3139.

(43) Iyer, R. P.; Egan, W.; Regan, J. B.; Beaucage, S. L. *J. Am. Chem. Soc.* **1990**, *112*, 1253–1254.

(44) Reed, M. W.; Adams, A. D.; Nelson, J. S.; Meyer, R. B., Jr. *Bioconjugate Chem.* **1991**, *2*, 217–225.

(45) Cantor, C. R.; Warshaw, M. M.; Shapiro, H. *Biopolymers* **1970**, *9*, 1059–1077.

for ODN conjugates or every 3 h for compound **8**. Analyses of the data were performed as described above.

**Determination of Sequence Specificity and Efficiency of DNA Alkylation by ODN Conjugates.** To determine efficiency and specificity of reaction between targeted hairpins and CPI- or MCPI-ODN conjugates, the hairpins were 5'-end-labeled with  $^{32}\text{P}$  using polynucleotide kinase and [ $\gamma$ - $^{32}\text{P}$ ]ATP. The  $^{32}\text{P}$ -labeled hairpin targets ( $2 \times 10^{-7}$  M) were mixed with reactive ODN derivatives ( $4 \times 10^{-7}$  M) in 140 mM KCl, 10 mM  $\text{MgCl}_2$ , and 20 mM HEPES (pH 7.2). The reactions (25  $\mu\text{L}$ ) were incubated at 37 °C. After 15 h, samples (1–2  $\mu\text{L}$ ) were mixed with 5–10  $\mu\text{L}$  of loading solution (8 M urea, 0.1% Bromophenol Blue, 0.1% Xylene Cyanole FF) and analyzed by electrophoresis on a denaturing polyacrylamide gel (~40 °C). Gels were transferred on a Whatman 3MM Chr paper (Whatman International Ltd, England) and dried *in vacuo*. The dried gels were visualized by autoradiography, and bands were quantified using a GS-250 Molecular Imager (Bio-Rad Laboratories, Inc., U.S.). Products of the cross-linking reactions were identified as slower migrating bands relatively to unmodified hairpin ODN. The yield of cross-linking reaction (%) or efficiency of alkylation was determined as the ratio between counts assigned to the products and total number of counts in the lane. To determine sequence specificity of alkylation, reactions

were incubated in boiling water for 30 min followed by treatment with 10% piperidine for 15 min at the same temperature. After the high-temperature treatment, reaction mixtures were dried using a SpeedVac, dissolved in 25–50  $\mu\text{L}$  of loading solution and analyzed by denaturing PAGE (55–60 °C). Statistical cleavage of each individual  $^{32}\text{P}$ -labeled ODN hairpin at the purine bases (A + G reaction; 60% formic acid, 37 °C, 12 min) was used as a control lane to assign detected bands of cleavage pattern to the bases of the targeted ODN hairpins which underwent alkylation.

**Acknowledgment.** We thank Dr. Alexander Gall for helpful discussions and computer modeling. A portion of this work was funded by Grant GM52774 from the National Institutes of Health, USPHS.

**Supporting Information Available:** Synthesis and characterization of **3–8**. Separation and characterization of diastereomers **4b,c** (8 pages). See any current masthead page for ordering and Internet access instructions.

JA9703133